Urinary volatile terpenes analyzed by gas chromatography-mass spectrometry to monitor breast cancer treatment efficacy in mice

Mark Woollam[1,2‡], Meghana Teli[1,3‡], Shengzhi Liu[1,3‡], Ali Daneshkhah[1], Amanda P. Siegel[1,2], Hiroki Yokota[1,3,4], and Mangilal Agarwal[1,2,5*]

[1]Integrated Nanosystems Development Institute, Indiana University-Purdue University, Indianapolis, 46202, USA

[2]Department of Chemistry and Chemical Biology, Indiana University-Purdue University Indianapolis, 46202, USA

[3]Department of Biomedical Engineering, Indiana University-Purdue University Indianapolis, 46202, USA

[4]Biomechanics and Biomaterials Research Center, Indianapolis, 46202, USA

[5]Department of Mechanical Engineering and Energy, Indiana University-Purdue University Indianapolis, 46202, USA

[*] Corresponding author: agarwal@iupui.edu, 317-278-9792, fax. 317-274-9744, 402 N. Blackford St., LD 326, Indianapolis, IN, 46202

[‡] Equally contributing authors

ABSTRACT: Urinary volatile terpene (VT) levels are significantly altered with induced models of breast cancer in mice. The question arises whether VTs can detect efficacy of anti-tumor treatments. BALB/c mice were injected with 4T1.2 murine tumor cells in the mammary pad or iliac artery to model localized breast cancer and induced bone metastasis. The effect of two dopaminergic anti-tumor agents was tested by conventional histology and altered VT levels. The headspace of urine specimens was analyzed by gas chromatography-mass spectrometry. In the localized model statistical significance ($p < 0.05$) was identified for 26% of VTs and in the metastasis model, 19% of VTs. The authors discovered separate VT panels classifying localized/control (area under the curve (AUC) = 1.0), and metastasis/control (AUC = 0.98). Treatment samples were tested using these panels and showed that mice treated with either agent were statistically significantly different than cancer samples, which is consistent with conventional analysis.

Keywords: Volatile organic compounds (VOCs), volatile terpenes (VTs), solid phase microextraction (SPME), gas chromatography (GC), mass spectrometry (MS), quadrupole time-of-flight (QTOF), principal component analysis (PCA), linear discriminant analysis (LDA), leave one out cross validation (LOOCV), area under the receiver operator characteristic (AUROC).

This is the author's manuscript of the article published in final edited form as:
Woollam, M., Teli, M., Liu, S., Daneshkhah, A., Siegel, A. P., Yokota, H., & Agarwal, M. (2020). Urinary Volatile Terpenes Analyzed by Gas Chromatography–Mass Spectrometry to Monitor Breast Cancer Treatment Efficacy in Mice. Journal of Proteome Research, 19(5), 1913-1922. https://doi.org/10.1021/acs.jproteome.9b00722

INTRODUCTION

Globally, cancer is the second most frequent cause of death after heart disorders. In 2020, over 30% of the estimated new cancer cases in women in the United States will be breast cancer and 15% of the estimated cancer related deaths in women will be caused by breast cancer[1]. Comprehensive breast cancer research has demonstrated its heterogeneous nature[2–4] through immunohistochemical markers and gene expression profiling[5]. Due to distinct tumor characteristics, cancers respond differentially to traditional treatments, making the "one model fits all" strategy imperfect. The growing knowledge about complexities of breast cancer pathogenesis demand tailoring personalized systemic and regional therapies to increase efficacy and decrease unnecessary morbidity[6]. Monitoring therapeutic effect can aid in patient decision-making throughout treatment and potentially help clinicians advance personalized medicine.

Molecular based methods for monitoring disease progression could include analysis of DNA[7], RNA[8], proteins[9–12], volatile organic compounds (VOCs)[13] and other metabolites[14–16]. VOCs are intermediates or final products of metabolic pathways and can provide potential information about disease[14]. They report not only intratumoral metabolism but also interactions between the tumor and its microenvironment[17]. VOCs are analyzed non-invasively from samples of urine, sweat, breath or other biological samples[18–20]. Different VOC biomarkers for various diseases have been proposed in previous studies[21–28]. It is anticipated that changes in VOC concentrations induced by cancer can be restored by therapeutic agents while their corresponding effect can be morphologically observed by measuring tumor size/weight.

Currently we are aware of no clinically established biomarkers solely dedicated for examining treatment effect for breast cancer. Diagnostic tests are usually extended for tracking therapeutic responses and corresponding tumor growth[29]. One of the common ways of assessing tumor size is through physical examination, but often results in incorrect prognosis[30]. Moreover, imaging methods such as PET, MRI and X-rays are expensive and have limitations in analyzing treatment induced morphological changes[31,32]. In addition, frequent use of these methods pose a potential harm of exposure to radiation[31]. Lastly, the evaluation of tumor size due to therapies is quantifiable only after about 6-8 weeks of treatment[33], which may be after the patient has received potentially harmful radiation/therapy for a prolonged period. Recent studies involving blood analysis of circulating tumor cells (CTCs) unveil a promising tool for determining treatment efficacy[34,35]. However, these studies may overlook the probability of clonal hematopoiesis[36]. Traditional metabolomic assays have identified potential markers for therapeutic efficacy[37,38], but efforts largely remain untargeted.

The authors previously reported that urinary VOC panels primarily comprised of volatile terpenes (VTs) were able to differentiate tumor-bearing mice from healthy control mice by headspace analysis coupled to gas chromatography-mass spectrometry quadrupole time-of-flight (GC-MS QTOF) and that a separate panel could differentiate between mice injected with tumors in the mammary pad from those injected in the bone[39]. Herein, the study is extended to determine if urinary VTs can non-invasively predict the effect of therapy on the tumor. The efficacy of two FDA approved agents involved in dopaminergic signalling, Trifluoperazine (TFP) and Fluphenazine (FP), were previously analyzed by CT, X-ray imaging and histological analysis of tumor size and weight[40]. Concurrently, urine was collected to understand the effect of these treatments on VT composition and corresponding correlation with metabolic pathways. This study demonstrates a novel approach through targeting VTs, by-products of the mevalonate pathway which has no known direct effect on dopaminergic metabolism, to detect cancer and monitor the efficacy of TFP and FP in mice.

EXPERIMENTAL SECTION

Materials and Reagents

Female BALB/c mice (~ 6 weeks of age) were purchased from Harlan Laboratories, Indianapolis, IN, USA. 4T1.2 tumor cells were obtained from Dr. R. Anderson at the Peter MacCallum Cancer Institute. Trifluoperazine dihydrochloride was purchased from Enzo (Cat. number: ALX-550-310-G001) and Fluphenazine dihydrochloride was purchased from Sigma Aldrich. Human urine standards were obtained from UTAK Laboratories, California. Two-centimeter polydimethylsiloxane/carboxen/divinylbenzene (PDMS/CAR/DVB) solid phase microextraction (SPME) fibers manufactured by Supelco and 8M Guanidine Hydrochloride (pH=8.5) were purchased from Sigma Aldrich. 10 mL headspace vials and 18 mm magnetic lids were purchased from Thermo Scientific. SPME Injection Sleeves were purchased from Sigma Aldrich (ID: 0.75 mm). A 7890A GC system coupled to an Agilent 7200 Accurate-Mass QTOF MS system with a PAL autosampling system (CTC Analytics) was used to analyze VOCs. The column utilized was an Agilent HP-5ms, 5% phenyl methyl siloxane GC column of 30 meters in length, 250 μm internal diameter and 0.25 μm film thickness. MATLAB (R2018b; Math Works) was used to generate hierarchical heatmaps and Origin (OriginLabs, 2018) was utilized for principal component analysis (PCA) mapping to visualize patterns in the data.

Tumor Cell Injection and Treatment

In the localized tumor model, 4T1.2 cells (5.0×10^5 cells in 50 μl PBS) were subcutaneously injected into the mammary fat pad of BALB/c female mice. These were further classified into three groups with mice receiving vehicle control (PBS solution) and mice treated with TFP and FP (1mg/kg body weight). Agents were administered every day at the site of tumor cell injection, and mice were sacrificed on day 18. For the induced bone metastasis tumor model, BALB/c female mice were injected with 4T1.2 cells (1.0 ×

10^5 cells in 50 µl PBS) in the right iliac artery. One group received vehicle control (PBS solution) while the agents TFP and FP were given to the other two groups via intra-peritoneal injection (2mg/kg body weight), and all mice were sacrificed on day 17. Normal control urine was collected from the mice prior to injection with tumor cells. Urine collection was performed in two time periods, with the first time period collecting from mice injected with tumor cells in the mammary pad and the second from mice injected in the iliac artery[40]. A whole-body X-ray image was taken using a Faxitron radiographic system (Faxitron X-ray Co., Tucson, AZ, USA).

Urine Collection and Sample Preparation

All experimental procedures followed the Guiding Principles in the Care and Use of Animals supported by the American Physiological Society and approved by Indiana University Animal Care and Use Committee. Mice were housed in glass cages at room temperature (25˚C) and fed the same diet (mouse-chow *ad libitum)*. Mice were moved to a cage covered in parafilm and urine was collected using pre-cleaned glass Pasteur pipettes into pre-cleaned 10 mL glass headspace vials over dry ice and stored in a -80˚C freezer prior to GC-MS QTOF analysis. Urine aliquots of 75 µL were prepared from each sample and 8M guanidine hydrochloride (GHCl) was added in a 1:1 ratio at room temperature one hour before GC analysis.

SPME and GC-MS QTOF

Methods for effective headspace analysis of VOCs in mouse urine differs slightly from analysis of human urine. Mouse urine contains major urinary proteins (MUPs) that sequester VOCs in hydrophobic pockets[41]. A common denaturing agent is GHCl[41] and was utilized herein. Urine was heated and agitated at 250 rpm and 60˚C for 30 minutes in a 10 mL vial to release VOCs into the sample headspace. Next, the pre-conditioned SPME fiber was inserted through the septum of the vial for a 30-minute incubation period at the same temperature and agitation rate to concentrate VOCs from the headspace. The fiber was conditioned at 260 ˚C for ten minutes prior to the first sample every day, and 4 minutes between runs. After incubation, the SPME fiber was inserted into the GC inlet at 250 ˚C for two minutes to thermally desorb VOCs. The chromatographic protocol involved the oven temperature maintaining 40 °C for 2 minutes followed by a ramp to 100 °C at a rate of 8 °C/min, 15 °C/min ramp to 120 °C, 8 °C/min to 180 °C, 15 °C/min to 200°C and finally an 8 °C/min ramp to 260 °C. Due to the limited amount of urine collected from each mouse, only one aliquot was analyzed for each sample. Controls of standard urine (UTAK Laboratories) were run daily and demonstrated reproducible measurements over the course of the experiment. The mass spectrometry data have been deposited to the Chorus Archive (https://chorusproject.org/pages/dashboard.html#/projects/all/1639/experiments) with the data set identifier 1639: Breast Cancer Volatile Biomarker Discovery in Mice.

Data Pre-processing and Pre-treatment

GC-MS QTOF data was collected utilizing Agilent Mass Hunter software in centroid format. Deconvolution and spectral alignment of chromatographic peaks across all samples based on similarities of mass-to-charge (m/z) ratios and retention times was performed using Mass Hunter Quantitative Profinder (version B.08.00). A matrix of compounds with integrated signal values and retention times for every sample was generated. Silica-based VOCs were removed from the data matrix as these are characteristic of SPME fiber and column degradation products. MS Total Useful Signal (MSTUS) was calculated using the remaining compounds and applied to normalize the data and remove unwanted variation between samples[42]. MSTUS vales were auto-scaled (z-scored) to obtain a similar range of signals for all VOCs in the sample matrix.

Univariate Analysis

The two data sets were tested for Gaussian distributions using skewness and kurtosis with the accepted limits of less than 1.96[43,44]. Univariate analysis was performed as a filter[45] using a two-tail Student's T-test (p-value < 0.05) on the VOCs present in at least 60% of at least one sample class to screen for VOCs differentially excreted between cancer and control sample classes. The $\log_2$ Fold Change of metabolites between the cancer and control sample groups was plotted against statistical significance to generate volcano plots for both comparisons (localized/control and metastasized/control)[46]. Hierarchical clustering was undertaken to visually observe cancer induced changes in VOC concentrations. Hierarchical heatmaps were created by z-scoring MSTUS values for each VOC across all samples[47]. Compounds are grouped on the y axis based on their similarities in terms of VOC signals across all samples. Euclidean distance metrics and average linkages were utilized to generate the hierarchical tree.

Compound Identification

VTs and VOCs with p-value < 0.05 were identified using Mass Hunter Quantitative Profinder and Mass Hunter Unknown Analysis (version B.08.00) integrated with the NIST14 mass spectral library. Compounds in Profinder were found in Unknown Analysis using average retention times and mass spectra. Features identified with a match factor higher than 65 from the NIST library were initially identified. Preliminary confirmation of these compounds was performed by comparing the non-polar retention index (NPRI) given in NIST to an experimental NPRI calculated from the average retention time using an instrument specific curve developed using standards. If the theoretical and experimental NPRI values were within the range of 75 units, the compound was deemed tentatively identified. Multivariate analysis was only performed on VTs with a match factor of at least 70. Identified VTs were further categorized into three groups: (1) VTs identified and confirmed by SPME GC-MS analysis of pure standards, (2) VTs identified with NPRI deviation < 5% and (3) VTs identified with > 5% but < 10% deviation in NPRI. All VTs identified in this study

are listed and grouped in Supplementary Table S1 with their difference in NPRI (ΔNPRI), retention time (RT), top three m/z peaks and match factor provided by NIST. The preliminary identification of isoprene and limonene was verified by running pure standards.

Multivariate Analysis

PCA was performed using all VOCs with p-value < 0.05 between cancer and control sample groups to visualize global patterns and sample outliers[48,49]. In contrast, based on the previous research highlighting the dysregulation of the mevalonate pathway in cancer, only VTs were used to develop panels discriminating between cancer and no-cancer. The matrix of VTs was analyzed using forward feature selection[49] coupled with Linear Discriminant Analysis (iterative LDA) to distinguish between cancer and control groups. The panel producing maximum distance between the cancer and control samples via iterative LDA was selected until the panel gave perfect separation between groups (area under the receiver operating characteristic (AUROC) equal to one). Leave one out cross validation (LOOCV) was performed to test if the classification models are overfit[50]. The Variation Inflation Factor (VIF) was calculated to assess the degree of multicollinearity present in each classification model[51]. A VIF threshold value of 10 was employed to indicate a high degree of multicollinearity between predictor and response values[52]. Samples receiving treatment were tested to determine if the classification model could predict the efficacy of TFP and FP. Primary LDA scores separating cancer/control sample classes were used to quantify the effect of treatments. One-tail T-tests were performed on LDA scores to determine if there was a statistical difference between the two treatments and control/cancer sample classes.

RESULTS AND DISCUSSION

X-ray and Histological Analysis and Urine Collection

In a related study, the results of which were reported previously[40], 24 BALB/c mice were injected with 4T1.2 cells in the mammary fat pad, eight of which received no treatment, eight received the FP treatment agent and the other eight received the TFP treatment agent. A different set of 23 mice were injected with 4T1.2 cells in the iliac artery and seven received no treatment, nine received FP and seven received TFP. From these mice, 58 urine samples were collected (see Table 1) and analyzed by GC-MS QTOF as described to identify potential breast cancer VT biomarkers and determine their ability to monitor therapeutic efficacy of TFP and FP. For the localized model, tumors from treated and untreated mice were weighed and measured in size. Tumors injected in the mammary pad were significantly lighter and smaller in mice treated with TFP or FP relative to untreated mice (results previously published)[40]. For the bone metastasis model, a whole-body X-ray image was taken prior to euthanasia (Figure 1). Compared to the normal control, the placebo without any treatment presented bone damages in the distal femur and the proximal tibia. However, administration of FP and TFP suppressed tumor induced bone damages. The previously published analysis was conducted via CT

and showed tumor bearing mice treated with TFP or FP had increased trabecular bone thickness. Mechanical testing also showed that mice receiving treatment had increased femur stiffness[40].

Data Screening and Univariate Analysis

Translating urine samples to potential volatile biomarkers starts by deconvoluting sample chromatograms and aligning VOCs across all samples. This process generated a matrix comprising a total of 215 VOCs (27 VTs) present in 60% of at least one sample class in the localized model and a matrix comprised of 370 VOCs (36 VTs) for the induced bone metastasis model. The data had a normal distribution with z-score values for skewness and kurtosis within the accepted limits. Volcano plots for both cancer models (localized/control and metastasized/control) can be observed in Figure 2 (a) and (b). Student's T-test alone gave a total of 24 VOCs with p-value < 0.05 between control and localized samples (17 upregulated and 7 downregulated) and 30 between control and metastasized samples (9 upregulated and 21 downregulated). Due to the specific focus on terpenes, VTs differentially excreted with a p-value < 0.05 are listed in Table 2. The Table contains, for each VT: an abbreviation, a colloquial name and IUPAC name, CAS ID, p-value, regulation in cancer samples and the model of cancer the VT was detected in. VTs in Table 2 can be observed on the volcano plots with their associated abbreviation in red (upregulated in cancer) or green (downregulated in cancer). 12 of the 14 VTs reported in Table 2 were detected in 100% of at least one sample class (control or cancer). The other two VTs (safranal and geranial) were detected frequently in cancer samples ($> 85\%$) and were largely depleted in control samples ($\leq 20\%$).

To illustrate trends showing variations in individual samples, hierarchical clustering of all VOCs with p-value < 0.05 was undertaken. Heatmaps for both models of cancer are shown in Figure 3(a) and (b). VTs with p-value < 0.05 are identified on the y-axis using their abbreviations in Table 2. It can be observed in the localized model (Figure 3(a)), four VTs are upregulated in breast cancer and three are downregulated. Even though more terpenes were identified as upregulated in the cancer sample class, the upregulated VTs have higher intraclass variation when compared to downregulated terpenes. For the bone metastasized model, five terpenes are downregulated and two are upregulated. VTs both up and downregulated in the metastasized model show low intraclass variation and high interclass variation between cancer and control samples (Figure 3(b)). Individual VTs and VOCs with p-value $<$ 0.05 were analyzed to identify if any single VOC could separate cancer and control samples. For both models of cancer, a single volatile was able to perfectly differentiate between control and cancer samples (Figure 4). 3-ethyl-2,5-dimethylhexa-1,3-diene (abbreviated as HEX in Table 2) discriminated between localized cancer and control samples. Figure 4(a) depicts a box/whisker plot of normalized signals for HEX in control, cancer and treatment sample classes. However, treatment samples (FP and TFP) demonstrated a statistically significant difference relative to control and no difference when compared to the cancer sample class, suggesting HEX alone was an imperfect reflection of histological data. In the bone metastasis model of breast cancer, 1,3-octadiene perfectly distinguished cancer and control samples (Figure 4(b)). In this case, TFP but not FP was significantly different than the cancer sample class, and both were different relative to control. The two VOCs in Figure 4(a) and (b) perfectly distinguish cancer

and control, but do not reflect the morphological and X-ray analyses which showed that both treatments had a significant inhibitory effect on tumor growth. This suggests a multivariate approach should be utilized.

Multivariate Analysis

Multivariate analysis can be used to identify outliers efficiently, visualize data patterns, and quantify trends observed in multiple compounds filtered by univariate analysis. PCA was implemented using all the compounds with p-value < 0.05 (Student's T-test) to visualize global patterns and identify any potential sample outliers: both PCA plots demonstrated absence of sample outliers (Supplementary Figure S1). Supervised multivariate techniques were employed to find a set of VTs with the highest classification accuracy between control and cancer samples. Terpenes, precursors of cholesterol and steroids, were identified as potential biomarkers both in the localized and metastasized tumor models. These results are consistent with our previous experiment conducted for identifying tumor site specific VOCs[39]. Following *Xia et al.*, knowledge and data driven based feature selection methods were utilized for iterative LDA[53] by using all 27 VTs related to the mevalonate pathway. A panel of three VOCs (d-limonene, safranal and ocimene) distinguished between localized and no cancer samples with an AUROC of 1.0. A graphical representation of this panel, LDA-Local, can be seen in Figure 5(a). LOOCV was utilized to test if the classification model was overfit, and it produced an estimated AUROC of 1.0. The VIF calculated for predictor and response values was 4.55 (low), demonstrating non-collinearity. When tested, the co-clustering of treated samples was quantified by the primary LDA scores depicted in Figure 5(a) and can be seen in Figure 5(c). Both treatments (TFP and FP) clustered in between cancer/control samples and were statistically different than cancer in the direction of control samples, indicating an intermediate response reflective of the morphological analysis. VOCs did not predict the treated mice were particularly healthy, however. LDA scores of FP treated samples were statistically significantly different than control samples in the direction of cancer, and TFP was not statistically different than control but had a p-value = 0.057.

For the metastasized model, forward feature selection was performed on all 36 VTs in a similar fashion. Five LDA classification models were built and all separated control and cancer perfectly (AUROC = 1.0). The model chosen to test treatment samples had the highest LOOCV AUROC and consisted of the VTs most frequently selected by the algorithm or compounds detected in the most samples. The panel chosen, LDA-Meta, consisted of three VTs (irone, bisabolene and geranial) and provided perfect classification of control and metastasized samples (Figure 5(b)). LOOCV was applied and produced an AUROC of 0.98, demonstrating the model is not overfit. The VIF calculated for predictor and response values was 2.0, demonstrating non-collinearity. Treatment samples were tested using this panel and clustered in between cancer/control samples. The primary LDA scores were analyzed and both treatments were statistically significantly different than cancer in the direction of control, and control

in the direction of cancer (Figure 5(d)). This demonstrates an intermediary response in VTs which is consistent with the degree of tumor induced bone damages depicted in the X-ray analysis in Figure 1(a) and (b).

Metabolic Interpretation

One of the hallmarks of cancer is its deregulation of cellular energetics by manipulating metabolic pathways[54]. A unique finding of this study is the relatively large number of terpenes in VOCs with p-value < 0.05 between control and cancer groups: of 63 VTs found, 14 or almost one quarter were statistically different between control and cancer groups. VT biosynthesis is a descending step of the mevalonate pathway and a precursor to cholesterol synthesis. A plethora of terpenes are synthesized from the reactions between geranyl pyrophosphate (GPP) and farnesyl pyrophosphate (FPP), which produce the building blocks of steroids. Figure 6 illustrates the bone metastasis tumor injection model leading to the dysregulation of the mevalonate pathway and differential expression of urinary VTs. Figure 6 defines some, but by no means all the VTs downstream of GPP in the mevalonate pathway that have been identified in Table 2 as potentially useful to detect cancer. VTs are also produced by plants and in general present a problem as potential interferents because they are found in food. This might provide a challenge for human urine analysis but could be overcome by subjects avoiding food with high VT content prior to donating urine. In this study however, all mice were fed the same diet (mouse-chow *ad libitum*) and were kept in the same environment. No significant difference in food consumption was observed between control, tumor-bearing and treated mice, but it is a limitation of this study that mouse-chow food consumption was not tracked precisely and analysis for VT content of mouse-chow is not included. Differentially excreted compounds presented in Figure 2 and 3 include 2, 5-ditert-butylcyclohexa-2, 5-diene-1, 4-dione, p-menth-3-ene, limonene, pelargonic acid and decanal, which are known to be involved in the lipid peroxidation metabolic pathway[22,55,56].

There is an intriguing link between VTs as markers of cancer and potential treatments for cancer. For example, terpenes and terpenoids are known to have inhibitory action against cancer[57,58] and cholesterol itself has previously been reported to play a role in the development of certain cancers[59]. In a different study, the current authors correlated the dysregulation of urinary VTs to the upregulation of cholesterol in mice[60]. This is significant as both VTs and cholesterol are end- or byproducts of the mevalonate pathway. The authors acknowledge VTs may also be presenting themselves in the form of glucuronides as studies have shown the glucuronidation of exogenous terpenes[61]. VTs endogenously synthesized as cancer-related byproducts will, even if partially glucuronidated, also be excreted in the free form and may therefore be considered potential biomarkers. For example, Silva *et al.* detected 4-carene as a potential biomarker for breast cancer[22] and Khalid *et al.* detected dihydromyrcenol as a marker for prostate cancer in human urine[62], both in the free form.

Any drug treatment would be expected to cause a change in mouse urine, including a change in expressed VOCs. To narrow the focus from untargeted analysis of VOC differences caused by drug treatments, this research focused on VTs that are by-products of the mevalonate pathway which is known to be dysregulated by cancer[63]. Our previous publication implicated many VTs as potential biomarkers of breast cancer, which allowed us to target them to build models for classification in this assay. Through targeted feature selection, strong and stable models were built using biologically relevant features. An added benefit of analyzing VTs is that there is no known direct relationship between Fluphenazine and Trifluoperazine and the mevalonate pathway, although a previous report on the effect of Fluphenazine as a treatment for mammary carcinoma in rats showed a decrease in cholesterol and an increase in cholesterol esters[64]. An unrelated report showed that extended administration of Trifluoperazine caused a significant rise in serum cholesterol in rabbits[65]. These may demonstrate indirect relationships of these agents with the mevalonate pathway.

CONCLUSION

The results from this study correspond to the findings found in previous work for breast cancer in mice models and extend the use of the potential VT biomarkers to monitor therapeutic efficacy of Trifluoperazine and Fluphenazine. Many of the potential biomarkers found in the previous work[39] belonged to the mevalonate or lipid peroxidation metabolic pathway and are reported in this study. For the mammary pad model, nine of the VOCs with p-value < 0.05 were previously reported, including limonene, isoprene (previously identified as penta-1,4-diene), 1-octen-3-one and kusol (1,2,3,4-tetrahydroquinoline). Six of the volatiles that were identified with $p < 0.05$ in the bone model were previously identified as potential biomarkers (1-octen-3-ol, bisabolene, 2-hexanone, 2-pentanone, 2-ethyl-2-hexenal and 4,5-dimethyl-4-hex-en-3-one). Similar and discrete results are expected in this study because mice injected in the mammary pad were compared to control mice independent of mice injected in the bone and mice injected in the bone were analyzed independent of mice injected in the mammary pad. This study lays out a potential method for analyzing effects of cancer therapy by testing VTs in urine. However, the results are based on a small number of mice all fed the same chow and infected with the same tumor cells. Furthermore, SPME GC-MS assays are the golden standard for analyzing VOCs but are not appropriate for analyzing larger hydrophilic molecules including glucuronidated VTs which are better analyzed using other MS-based methods. It is anticipated it would be very beneficial to extend this promising approach to more heterogeneous samples and larger data sets. Optimization of urine collection/preparation and analytical techniques may improve the identification and discovery of VT biomarkers in patient samples.

SUPPORTING INFORMATION

Table S1. Volatile Terpenes reported in this study with percent differences in NPRI, retention time (RT), top three m/z peaks and NIST match factor.

Figure S1. Principle Component Analysis of statistically significant (p-value < 0.05) VOCs in control, tumor and treatment models for (a) localized and (b) metastasized breast cancer.

AUTHOR INFORMATION

Corresponding Author

*agarwal@iupui.edu, 317-278-9792, fax. 317-274-9744, 402 N. Blackford St., LD 326, Indianapolis, IN, 46202

Author Contributions

‡M. Woollam, M. Teli and S. Liu contributed equally. M. Agarwal, A.P. Siegel and H. Yokota designed the experiments used in this study. S Liu and H. Yokota injected the tumor cells in the mice and collected their urine. H. Yokota and S. Liu analyzed tumor induced bone damages via X-ray imaging. M. Woollam and M. Teli aliquoted and prepared the mouse urine samples and analyzed the samples via GC-MS QTOF. M. Woollam, M. Teli, A.P. Siegel, A. Daneshkhah, H. Yokota and M. Agarwal performed data screening, all the statistical analysis, and wrote the manuscript. All authors reviewed the manuscript.

ACKNOWLEDGMENT

The authors would like to thank Solveig Naumann for optimization of procedure and Paula Angarita-Rivera for assisting with analyzing urine samples via GC-MS QTOF. The authors would finally like to acknowledge the National Science Foundation (grant # 1502310) and Agilent Technologies. The author(s) declare no financial or other competing interests.

.

REFERENCES

(1) Siegel, R. L.; Miller, K. D.; Jemal, A. Cancer Statistics, 2019. *CA: A Cancer Journal for Clinicians* **2019**, *69* (1), 7–34. https://doi.org/10.3322/caac.21551.

(2) Marusyk, A.; Polyak, K. Tumor Heterogeneity: Causes and Consequences. *Biochim Biophys Acta* **1805**, *2010*.

(3) Potter, J. D.; Cerhan, J. R.; Sellers, T. A.; McGovern, P. G.; Drinkard, C.; Kushi, L. R.; Folsom, A. R. Progesterone and Estrogen Receptors and Mammary Neoplasia in the Iowa Women's Health Study: How Many Kinds of Breast Cancer Are There? *Cancer Epidemiol Biomarkers Prev* **1995**, *4* (4), 319.

(4) Martelotto, L. G.; Ng, C. K.; Piscuoglio, S.; Weigelt, B.; Reis-Filho, J. S. Breast Cancer Intra-Tumor Heterogeneity. *Breast Cancer Research* **2014**, *16* (3), 210. https://doi.org/10.1186/bcr3658.
(5) Coleman, W. B.; Tsongalis, G. J. *Molecular Pathology: The Molecular Basis of Human Disease*; Academic Press: Cambridge, MA, 2017; 2nd edition, pp 136-148.
(6) Coates, A. S.; Winer, E. P.; Goldhirsch, A.; Gelber, R. D.; Gnant, M.; Piccart-Gebhart, M.; Thürlimann, B.; Senn, H.-J. Tailoring Therapies—Improving the Management of Early Breast Cancer: St Gallen International Expert Consensus on the Primary Therapy of Early Breast Cancer 2015. *Ann Oncol* **2015**, *26* (8), 1533–1546. https://doi.org/10.1093/annonc/mdv221.
(7) Li, S.-X.; Sjolund, A.; Harris, L.; Sweasy, J. B. DNA Repair and Personalized Breast Cancer Therapy. *Environ Mol Mutagen* **2010**, *51* (8–9), 897–908. https://doi.org/10.1002/em.20606.
(8) Umelo, I. A.; Costanza, B.; Castronovo, V. Innovative Methods for Biomarker Discovery in the Evaluation and Development of Cancer Precision Therapies. *Cancer and Metastasis Reviews* **2018**, *37* (1), 125–145. https://doi.org/10.1007/s10555-017-9710-0.
(9) Gam, L.-H. Breast Cancer and Protein Biomarkers. *World J Exp Med* **2012**, *2* (5), 86–91. https://doi.org/10.5493/wjem.v2.i5.86.
(10) Zamay, T. N.; Zamay, G. S.; Kolovskaya, O. S.; Zukov, R. A.; Petrova, M. M.; Gargaun, A.; Berezovski, M. V.; Kichkailo, A. S. Current and Prospective Protein Biomarkers of Lung Cancer. *Cancers (Basel)* **2017**, *9* (11). https://doi.org/10.3390/cancers9110155.
(11) Ou, K.; Yu, K.; Kesuma, D.; Hooi, M.; Huang, N.; Chen, W.; Lee, S. Y.; Goh, X. P.; Tan, L. keng; Liu, J.; et al. Novel Breast Cancer Biomarkers Identified by Integrative Proteomic and Gene Expression Mapping. *J. Proteome Res.* **2008**, *7* (4), 1518–1528. https://doi.org/10.1021/pr700820g.
(12) Chen, I.-H.; Aguilar, H. A.; Paez Paez, J. S.; Wu, X.; Pan, L.; Wendt, M. K.; Iliuk, A. B.; Zhang, Y.; Tao, W. A. Analytical Pipeline for Discovery and Verification of Glycoproteins from Plasma-Derived Extracellular Vesicles as Breast Cancer Biomarkers. *Anal. Chem.* **2018**, *90* (10), 6307–6313. https://doi.org/10.1021/acs.analchem.8b01090.
(13) Chen, Y.; Zhang, Y.; Pan, F.; Liu, J.; Wang, K.; Zhang, C.; Cheng, S.; Lu, L.; Zhang, W.; Zhang, Z.; et al. Breath Analysis Based on Surface-Enhanced Raman Scattering Sensors Distinguishes Early and Advanced Gastric Cancer Patients from Healthy Persons. *ACS Nano* **2016**, *10* (9), 8169–8179. https://doi.org/10.1021/acsnano.6b01441.
(14) Wu, W.; Zhao, S. Metabolic Changes in Cancer: Beyond the Warburg Effect. *Acta Biochimica et Biophysica Sinica* **2013**, *45* (1), 18–26. https://doi.org/10.1093/abbs/gms104.
(15) Wang, R.; Zhao, H.; Zhang, X.; Zhao, X.; Song, Z.; Ouyang, J. Metabolic Discrimination of Breast Cancer Subtypes at the Single-Cell Level by Multiple Microextraction Coupled with Mass Spectrometry. *Anal. Chem.* **2019**, *91* (5), 3667–3674. https://doi.org/10.1021/acs.analchem.8b05739.
(16) Guo, M.; Zhang, L.; Du, Y.; Du, W.; Liu, D.; Guo, C.; Pan, Y.; Tang, D. Enrichment and Quantitative Determination of 5-(Hydroxymethyl)-2′-Deoxycytidine, 5-(Formyl)-2′-Deoxycytidine, and 5-(Carboxyl)-2′-Deoxycytidine in Human Urine of Breast Cancer Patients by Magnetic Hyper-Cross-Linked Microporous Polymers Based on Polyionic Liquid. *Anal. Chem.* **2018**, *90* (6), 3906–3913. https://doi.org/10.1021/acs.analchem.7b04755.
(17) Giussani, M.; Merlino, G.; Cappelletti, V.; Tagliabue, E.; Daidone, M. G. Tumor-Extracellular Matrix Interactions: Identification of Tools Associated with Breast Cancer Progression. *Seminars in Cancer Biology* **2015**, *35*, 3–10. https://doi.org/10.1016/j.semcancer.2015.09.012.
(18) Greenberg, A. K.; Lee, M. S. Biomarkers for Lung Cancer: Clinical Uses. *Current Opinion in Pulmonary Medicine* **2007**, *13* (4), 249–255. https://doi.org/10.1097/MCP.0b013e32819f8f06.
(19) Sànchez, M. N.; García, E.H.; Pavón, J.L.; Cordero, B.M.; Fast Analytical Methodology Based on Mass Spectrometry for the Determination of Volatile Biomarkers in Saliva, *Anal. Chem.* **2012**, 84(1): 379-85 https://pubs.acs.org/doi/abs/10.1021/ac2026892.

(20) Bosch, S.; el Manouni el Hassani, S.; Covington, J. A.; Wicaksono, A. N.; Bomers, M. K.; Benninga, M. A.; Mulder, C. J. J.; de Boer, N. K. H.; de Meij, T. G. J. Optimized Sampling Conditions for Fecal Volatile Organic Compound Analysis by Means of Field Asymmetric Ion Mobility Spectrometry. *Anal. Chem.* **2018**, *90* (13), 7972–7981. https://doi.org/10.1021/acs.analchem.8b00688.

(21) Lavra, L.; Catini, A.; Ulivieri, A.; Capuano, R.; Baghernajad Salehi, L.; Sciacchitano, S.; Bartolazzi, A.; Nardis, S.; Paolesse, R.; Martinelli, E.; et al. Investigation of VOCs Associated with Different Characteristics of Breast Cancer Cells. *Scientific Reports* **2015**, *5*, 13246.

(22) Silva, C. L.; Passos, M.; Câmara, J. S. Solid Phase Microextraction, Mass Spectrometry and Metabolomic Approaches for Detection of Potential Urinary Cancer Biomarkers—A Powerful Strategy for Breast Cancer Diagnosis. *Talanta* **2012**, *89*, 360–368. https://doi.org/10.1016/j.talanta.2011.12.041.

(23) Hanai, Y.; Shimono, K.; Oka, H.; Baba, Y.; Yamazaki, K.; Beauchamp, G. K. Analysis of Volatile Organic Compounds Released from Human Lung Cancer Cells and from the Urine of Tumor-Bearing Mice. *Cancer Cell International* **2012**, *12* (1), 7. https://doi.org/10.1186/1475-2867-12-7.

(24) Siegel, A. P.; Daneshkhah, A.; Hardin, D. S.; Shrestha, S.; Varahramyan, K.; Agarwal, M. Analyzing Breath Samples of Hypoglycemic Events in Type 1 Diabetes Patients: Towards Developing an Alternative to Diabetes Alert Dogs. *Journal of Breath Research* **2017**, *11* (2), 026007. https://doi.org/10.1088/1752-7163/aa6ac6.

(25) Phillips, M. Method for the Collection and Assay of Volatile Organic Compounds in Breath. *Analytical Biochemistry* **1997**, *247* (2), 272–278. https://doi.org/10.1006/abio.1997.2069.

(26) Phillips, M.; Herrera, J.; Krishnan, S.; Zain, M.; Greenberg, J.; Cataneo, R. N. Variation in Volatile Organic Compounds in the Breath of Normal Humans. *Journal of Chromatography B: Biomedical Sciences and Applications* **1999**, *729* (1), 75–88. https://doi.org/10.1016/S0378-4347(99)00127-9.

(27) Banday, K. M.; Pasikanti, K. K.; Chan, E. C. Y.; Singla, R.; Rao, K. V. S.; Chauhan, V. S.; Nanda, R. K. Use of Urine Volatile Organic Compounds To Discriminate Tuberculosis Patients from Healthy Subjects. *Anal. Chem.* **2011**, *83* (14), 5526–5534. https://doi.org/10.1021/ac200265g.

(28) Huang, J.; Kumar, S.; Abbassi-Ghadi, N.; Španěl, P.; Smith, D.; Hanna, G. B. Selected Ion Flow Tube Mass Spectrometry Analysis of Volatile Metabolites in Urine Headspace for the Profiling of Gastro-Esophageal Cancer. *Anal. Chem.* **2013**, *85* (6), 3409–3416. https://doi.org/10.1021/ac4000656.

(29) Diagnostic & Monitoring Tests | Cancer Testing | UNM Cancer Center http://cancer.unm.edu/cancer/cancer-info/testing-overview/diagnostics-monitoring-tests/ (accessed Feb 9, 2019).

(30) Bevers, T. B.; Helvie, M.; Bonaccio, E.; Calhoun, K. E.; Daly, M. B.; Farrar, W. B.; Garber, J. E.; Gray, R.; Greenberg, C. C.; Greenup, R.; et al. Breast Cancer Screening and Diagnosis, Version 3.2018, NCCN Clinical Practice Guidelines in Oncology. *Journal of the National Comprehensive Cancer Network* **2018**, *16* (11), 1362–1389. https://doi.org/10.6004/jnccn.2018.0083.

(31) Radhakrishna, S.; Agarwal, S.; Parikh, P. M.; Kaur, K.; Panwar, S.; Sharma, S.; Dey, A.; Saxena, K. K.; Chandra, M.; Sud, S. Role of Magnetic Resonance Imaging in Breast Cancer Management. *South Asian J Cancer* **2018**, *7* (2), 69–71. https://doi.org/10.4103/sajc.sajc_104_18.

(32) Egan, T. K. Monitoring Patients Undergoing Cancer Therapy. *Laboratory Medicine* **2000**, *31* (12), 666–671. https://doi.org/10.1309/R078-Y40Q-PAJP-1RPP.

(33) Thoeny, H. C.; Ross, B. D. Predicting and Monitoring Cancer Treatment Response with DW-MRI. *J Magn Reson Imaging* **2010**, *32* (1), 2–16. https://doi.org/10.1002/jmri.22167.

(34) Dawson, S.-J.; Tsui, D. W. Y.; Murtaza, M.; Biggs, H.; Rueda, O. M.; Chin, S.-F.; Dunning, M. J.; Gale, D.; Forshew, T.; Mahler-Araujo, B.; et al. Analysis of Circulating Tumor DNA to Monitor Metastatic Breast Cancer. *N Engl J Med* **2013**, *368* (13), 1199–1209. https://doi.org/10.1056/NEJMoa1213261.

(35) Rothé, F.; Laes, J.-F.; Lambrechts, D.; Smeets, D.; Vincent, D.; Maetens, M.; Fumagalli, D.; Michiels, S.; Drisis, S.; Moerman, C.; et al. Plasma Circulating Tumor DNA as an Alternative to Metastatic Biopsies for Mutational Analysis in Breast Cancer. *Ann Oncol* **2014**, *25* (10), 1959–1965. https://doi.org/10.1093/annonc/mdu288.

(36) Razavi, P.; Li, B. T.; Hou, C.; Shen, R.; Venn, O.; Lim, R. S.; Hubbell, E.; De Bruijn, I.; Liu, Q.; Vijaya Satya, R.; et al. Cell-Free DNA (CfDNA) Mutations from Clonal Hematopoiesis: Implications for Interpretation of Liquid Biopsy Tests. *JCO* **2017**, *35* (15_suppl), 11526–11526. https://doi.org/10.1200/JCO.2017.35.15_suppl.11526.

(37) Armitage, E. G.; Southam, A. D. Monitoring Cancer Prognosis, Diagnosis and Treatment Efficacy Using Metabolomics and Lipidomics. *Metabolomics* **2016**, *12* (9), 146. https://doi.org/10.1007/s11306-016-1093-7.

(38) Shi, J.; Cao, B.; Wang, X.-W.; Aa, J.-Y.; Duan, J.-A.; Zhu, X.-X.; Wang, G.-J.; Liu, C.-X. Metabolomics and Its Application to the Evaluation of the Efficacy and Toxicity of Traditional Chinese Herb Medicines. *Journal of Chromatography B* **2016**, *1026*, 204–216. https://doi.org/10.1016/j.jchromb.2015.10.014.

(39) Woollam, M.; Teli, M.; Angarita-Rivera, P.; Liu, S.; Siegel, A. P.; Yokota, H.; Agarwal, M. Detection of Volatile Organic Compounds (VOCs) in Urine via Gas Chromatography-Mass Spectrometry QTOF to Differentiate Between Localized and Metastatic Models of Breast Cancer. *Scientific Reports* **2019**, *9* (1), 2526. https://doi.org/10.1038/s41598-019-38920-0.

(40) Liu, S.; Fan, Y.; Chen, A.; Jalali, A.; Minami, K.; Ogawa, K.; Nakshatri, H.; Li, B.-Y.; Yokota, H. Osteocyte-Driven Downregulation of Snail Restrains Effects of Drd2 Inhibitors on Mammary Tumor Cells. *Cancer Res* **2018**, *78* (14), 3865. https://doi.org/10.1158/0008-5472.CAN-18-0056.

(41) Kwak, J.; Grigsby, C. C.; Rizki, M. M.; Preti, G.; Köksal, M.; Josue, J.; Yamazaki, K.; Beauchamp, G. K. Differential Binding between Volatile Ligands and Major Urinary Proteins Due to Genetic Variation in Mice. *Physiology & Behavior* **2012**, *107* (1), 112–120. https://doi.org/10.1016/j.physbeh.2012.06.008.

(42) Li, B.; Tang, J.; Yang, Q.; Li, S.; Cui, X.; Li, Y.; Chen, Y.; Xue, W.; Li, X.; Zhu, F. NOREVA: Normalization and Evaluation of MS-Based Metabolomics Data. *Nucleic Acids Res* **2017**, *45* (Web Server issue), W162–W170. https://doi.org/10.1093/nar/gkx449.

(43) Ghasemi, A.; Zahediasl, S. Normality Tests for Statistical Analysis: A Guide for Non-Statisticians. *Int J Endocrinol Metab* **2012**, *10* (2), 486–489. https://doi.org/10.5812/ijem.3505.

(44) Kim, H.-Y. Statistical Notes for Clinical Researchers: Assessing Normal Distribution (2) Using Skewness and Kurtosis. *Restor Dent Endod* **2013**, *38* (1), 52–54. https://doi.org/10.5395/rde.2013.38.1.52.

(45) Saccenti, E.; Hoefsloot, H. C. J.; Smilde, A. K.; Westerhuis, J. A.; Hendriks, M. M. W. B. Reflections on Univariate and Multivariate Analysis of Metabolomics Data. *Metabolomics* **2014**, *10* (3), 361–374. https://doi.org/10.1007/s11306-013-0598-6.

(46) Kumar, N.; Hoque, Md. A.; Sugimoto, M. Robust Volcano Plot: Identification of Differential Metabolites in the Presence of Outliers. *BMC Bioinformatics* **2018**, *19* (1), 128. https://doi.org/10.1186/s12859-018-2117-2.

(47) Murtagh, F.; Contreras, P. Algorithms for Hierarchical Clustering: An Overview, II. *Wiley Interdisciplinary Reviews: Data Mining and Knowledge Discovery* **2017**, *7* (6), e1219. https://doi.org/10.1002/widm.1219.

(48) Liu, Y.; Vincenti, M. P.; Yokota, H. Principal Component Analysis for Predicting Transcription-Factor Binding Motifs from Array-Derived Data. *BMC Bioinformatics* **2005**, *6* (1), 276. https://doi.org/10.1186/1471-2105-6-276.

(49) Xia, J.; Broadhurst, D. I.; Wilson, M.; Wishart, D. S. Translational Biomarker Discovery in Clinical Metabolomics: An Introductory Tutorial. *Metabolomics* **2013**, *9* (2), 280–299. https://doi.org/10.1007/s11306-012-0482-9.

(50) Babyak, M. A. What You See May Not Be What You Get: A Brief, Nontechnical Introduction to Overfitting in Regression-Type Models. *Psychosom. Med.* **2004**, *66* (3), 411-21. https://doi.org/10.1097/01.psy.0000127692.23278.a9.

(51) Belsley, D. A. A Guide to Using the Collinearity Diagnostics. *Computer Science in Economics and Management* **1991**, *4* (1), 33–50. https://doi.org/10.1007/BF00426854.

(52) Hair, J.F.; Black, W.C., Babin, B.J.; Anderson, R.E.*; Multivariate Data Analysis,* Pearson New International Edition; Pearson: Harlow, 2014; 7th edition, pp 195-201.

(53) He, Z.; Yu, W. Stable Feature Selection for Biomarker Discovery. *Computational Biology and Chemistry* **2010**, *34* (4), 215–225. https://doi.org/10.1016/j.compbiolchem.2010.07.002.

(54) Hanahan, D.; Weinberg, R. A. Hallmarks of Cancer: The Next Generation. *Cell* **2011**, *144* (5), 646–674. https://doi.org/10.1016/j.cell.2011.02.013.

(55) Wishart, D. S.; Feunang, Y. D.; Marcu, A.; Guo, A. C.; Liang, K.; Vázquez-Fresno, R.; Sajed, T.; Johnson, D.; Li, C.; Karu, N.; et al. HMDB 4.0: The Human Metabolome Database for 2018. *Nucleic Acids Res* **2018**, *46* (Database issue), D608–D617. https://doi.org/10.1093/nar/gkx1089.

(56) Altomare, D. F.; Di Lena, M.; Porcelli, F.; Trizio, L.; Travaglio, E.; Tutino, M.; Dragonieri, S.; Memeo, V.; de Gennaro, G. Exhaled Volatile Organic Compounds Identify Patients with Colorectal Cancer. *BJS* **2013**, *100* (1), 144–150. https://doi.org/10.1002/bjs.8942.

(57) Gould M N. Cancer Chemoprevention and Therapy by Monoterpenes. *Environmental Health Perspectives* **1997**, *105* (suppl 4), 977–979. https://doi.org/10.1289/ehp.97105s4977.

(58) Paduch, R.; Kandefer-Szerszeń, M.; Trytek, M.; Fiedurek, J. Terpenes: Substances Useful in Human Healthcare. *Archivum Immunologiae et Therapiae Experimentalis* **2007**, *55* (5), 315. https://doi.org/10.1007/s00005-007-0039-1.

(59) Llaverias, G.; Danilo, C.; Mercier, I.; Daumer, K.; Capozza, F.; Williams, T. M.; Sotgia, F.; Lisanti, M. P.; Frank, P. G. Role of Cholesterol in the Development and Progression of Breast Cancer. *Am J Pathol* **2011**, *178* (1), 402–412. https://doi.org/10.1016/j.ajpath.2010.11.005.

(60) Wang, L.; Wang, Y.; Chen, A.; Teli, M.; Kondo, R.; Jalali, A.; Fan, Y.; Liu, S.; Zhao, X.; Siegel, A.; et al. Pitavastatin Slows Tumor Progression and Alters Urine-Derived Volatile Organic Compounds through the Mevalonate Pathway. *FASEB J.* **2019**, *33* (12), 13710–13721. https://doi.org/10.1096/fj.201901388R.

(61) Poon, G. K.; Vigushin, D.; Griggs, L. J.; Rowlands, M. G.; Coombes, R. C.; Jarman, M. Identification and Characterization of Limonene Metabolites in Patients with Advanced Cancer by Liquid Chromatography/Mass Spectrometry. *Drug Metab. Dispos.* **1996**, *24* (5), 565–571.

(62) Khalid, T.; Aggio, R.; White, P.; De Lacy Costello, B.; Persad, R.; Al-Kateb, H.; Jones, P.; Probert, C. S.; Ratcliffe, N. Urinary Volatile Organic Compounds for the Detection of Prostate Cancer. *PLoS ONE* **2015**, *10* (11), e0143283. https://doi.org/10.1371/journal.pone.0143283.

(63) Mullen, P. J.; Yu, R.; Longo, J.; Archer, M. C.; Penn, L. Z. The Interplay between Cell Signalling and the Mevalonate Pathway in Cancer. *Nature Reviews Cancer* **2016**, *16* (11), 718–731. https://doi.org/10.1038/nrc.2016.76.

(64) Hilf, R.; Bell, C.; Goldenberg, H.; Michel, I. Effect of Fluphenazine HC1 on R3230AC Mammary Carcinoma and Mammary Glands of the Rat. **1971**, *31*, 8.

(65) Bala, S.; Garg, K. N. Effect of Prolonged Trifluoperazine, Imipramine and Haloperidol Administration on Serum Cholesterol. *Pharmacology* **1976**, *14* (5), 385–389. https://doi.org/10.1159/000136619.

Table 1. Number of mice from each model of breast cancer

Model	Treatment	Number of mice
Mammary pad (localized)	Control	5
	Cancer	8
	Fluphenazine	8
	Trifluoperazine	8
Induced bone metastasis (metastasized)	Control	6
	Cancer	7
	Fluphenazine	9
	Trifluoperazine	7

Table 2. Chemical names of volatile terpenes with p-value <0.05 for both cancer models

Abbreviation	IUPAC (Common Names)	CAS ID	P-value	Regulation	Cancer Model
LIM	(4R)-1-methyl-4-prop-1-en-2-ylcyclohexene (Limonene)	5989-27-5	0.013	down	Localized
SAF	2,6,6-trimethylcyclohexa-1,3-diene-1-carbaldehyde (Safranal)	116-26-7	0.014	up	Localized
MEN	4-methyl-1-propan-2-ylcyclohexene (p-Menth-3-ene)	500-00-5	0.015	up	Localized
HEX	3-ethyl-2,5-dimethylhexa-1,3-diene	61142-36-7	0.017	up	Localized
BIC	1-methoxy-4-methylbicyclo[2.2.2]octane	6555-95-9	0.021	up	Localized
ISO	2-methylbuta-1,3-diene (Isoprene)	78-79-5	0.032	down	Localized
ISA	2-methylbut-3-en-2-ol (Isoprenyl Alcohol)	115-18-4	0.044	down	Localized
CRY	4-propan-2-ylcyclohex-2-en-1-one (Crypton)	500-02-7	0.009	down	Metastasized
THU	2-hydroxy-5-propan-2-ylcyclohepta-2,4,6-trien-1-one (Thujaplicin)	672-76-4	0.013	down	Metastasized
GER	3,7-dimethylocta-2,6-dienal (Geranial)	141-27-5	0.013	up	Metastasized
BIS	1-methyl-4-(6-methylhepta-1,5-dien-2-yl)cyclohexene (Bisabolene)	495-61-4	0.014	down	Metastasized
IRO	4-(2,5,6,6-tetramethylcyclohex-2-en-1-yl)but-3-en-2-one (Irone)	79-69-6	0.031	down	Metastasized
NER	3,7-dimethylocta-2,6-dien-1-ol (Nerol)	106-25-2	0.036	up	Metastasized
CYU	1,5,9,9-tetramethylcycloundeca-1,4,7-triene	NA	0.037	down	Metastasized

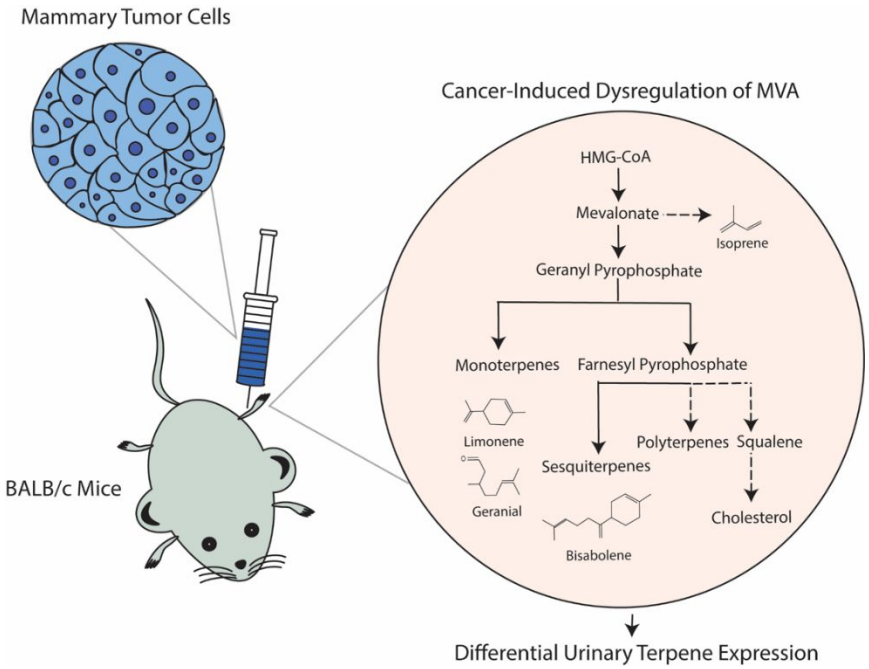
Mammary Tumor Cells
BALB/c Mice
Cancer-Induced Dysregulation of MVA
HMG-CoA
Mevalonate
Isoprene
Geranyl Pyrophosphate
Monoterpenes
Farnesyl Pyrophosphate
Limonene
Polyterpenes
Squalene
Sesquiterpenes
Geranial
Cholesterol
Bisabolene
Differential Urinary Terpene Expression

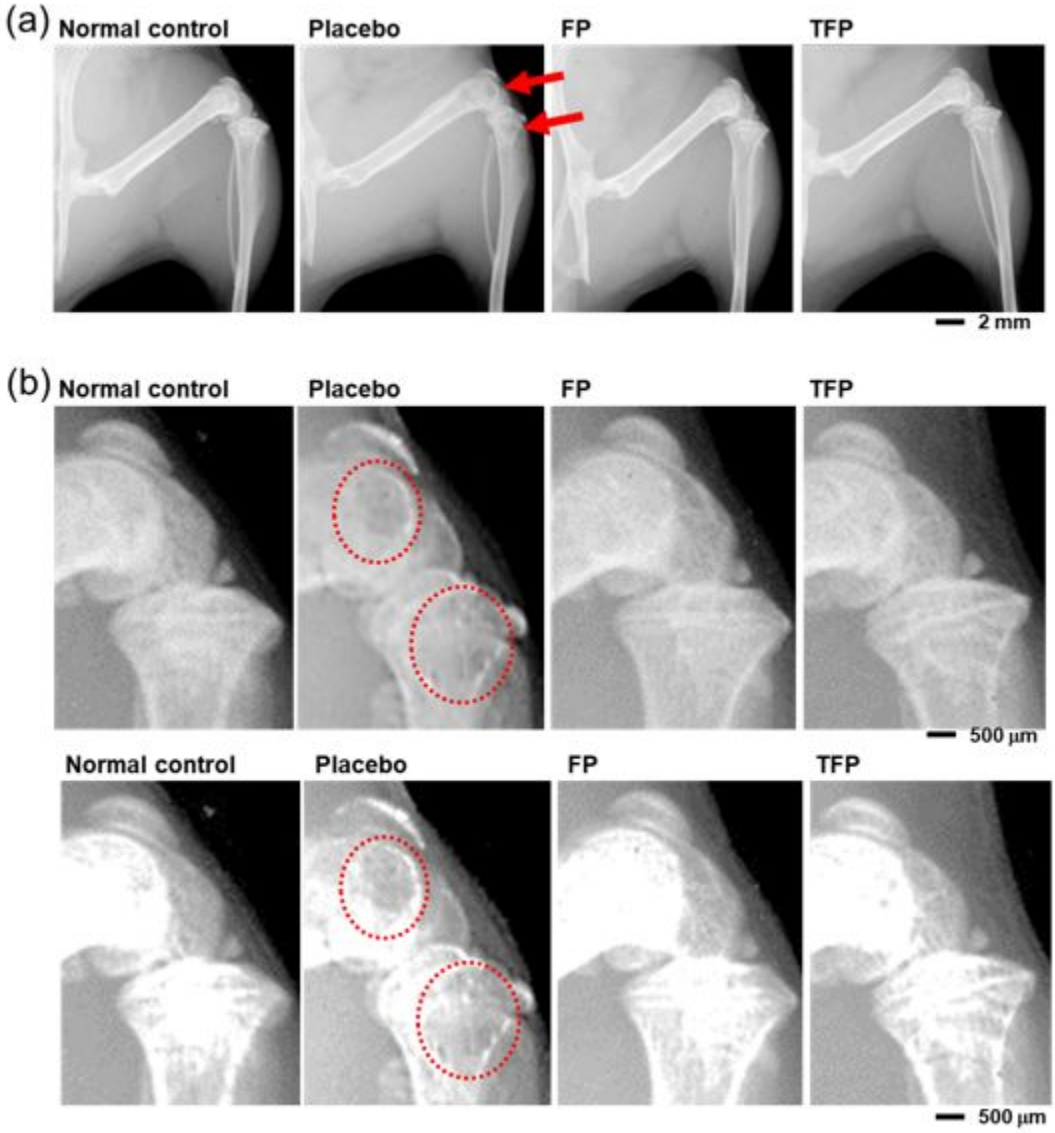

Figure 1. X-ray images of the distal femur and proximal tibia in the bone metastasis model for the left hindlimb (a) and the knee (b). The red arrows in (a) and red circles in (b) indicate tumor-induced bone damages, and the knee images are shown in two X-ray levels (low and high).

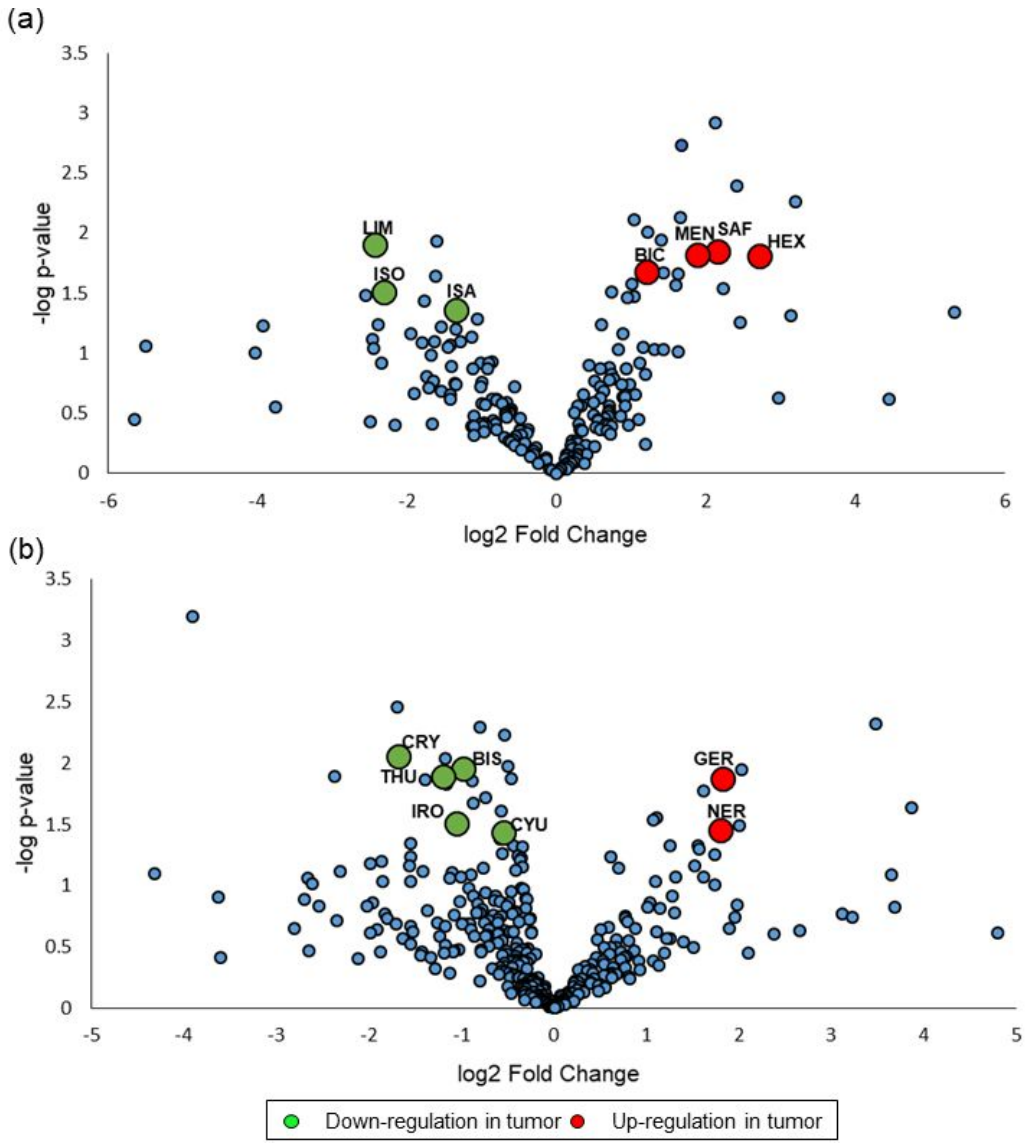

Figure 2. Volcano plots for (a) control/localized and (b) control/metastasized tumor models with negative log of p-value from Students T-test plotted as a function of log2 Fold Change (VTs in Table 2 with p-value < 0.05 are labeled and highlighted in green or red).

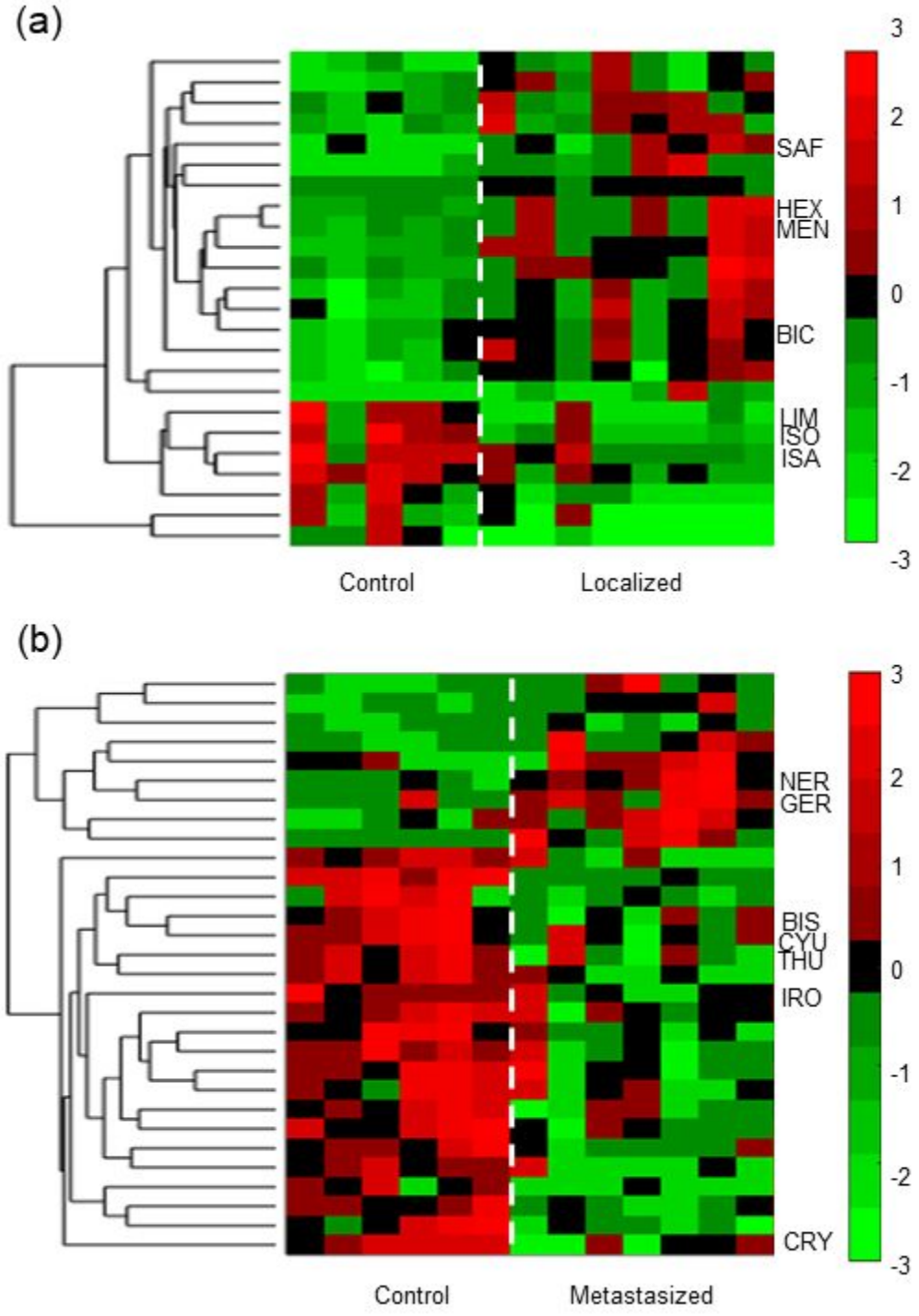

Figure 3. Hierarchical clustering of VOCs with p-value < 0.05 in control and tumor samples to visualize and observe the change in concentration for (a) localized and (b) metastasized models of breast cancer. VTs with p-value < 0.05 are labeled using their corresponding abbreviation in Table 2.

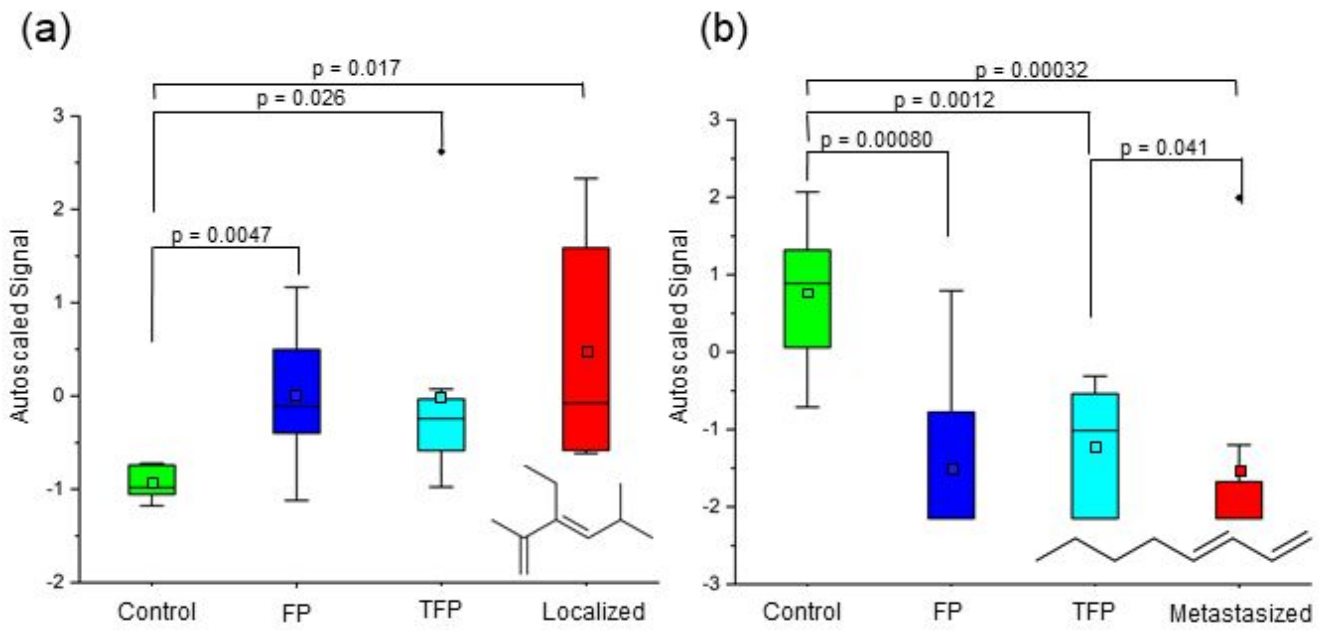

Figure 4. Box and whisker plots using normalized signals for (a) 3-ethyl-2,5-dimethylhexa-1,3-diene in the localized model and (b) 1,3-octadiene in the metastasized model of breast cancer (average values are colored squares and sample outliers are black diamonds).

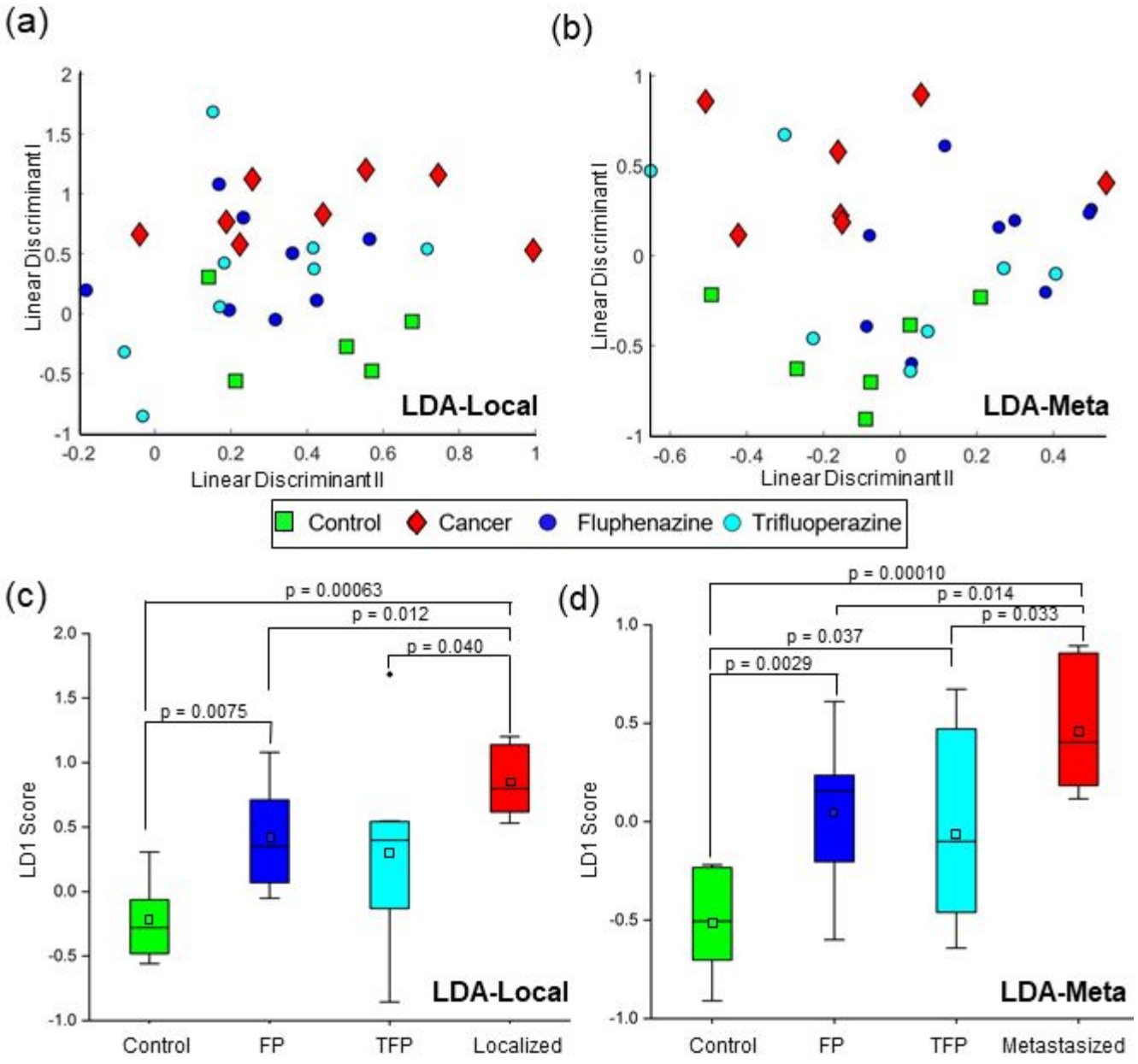

Figure 5. Linear discriminant analysis (LDA) plot (a) utilizing limonene, safranal and ocimene to discriminate localized and control sample classes and test treatment samples and (b) using irone, bisabolene and geranial to separate metastasized/control samples and test treated urine. Box/whisker plots of the primary LDA scores for all sample classes in the (c) localized model and (d) bone metastasis model (average values are colored squares and sample outliers are black diamonds).

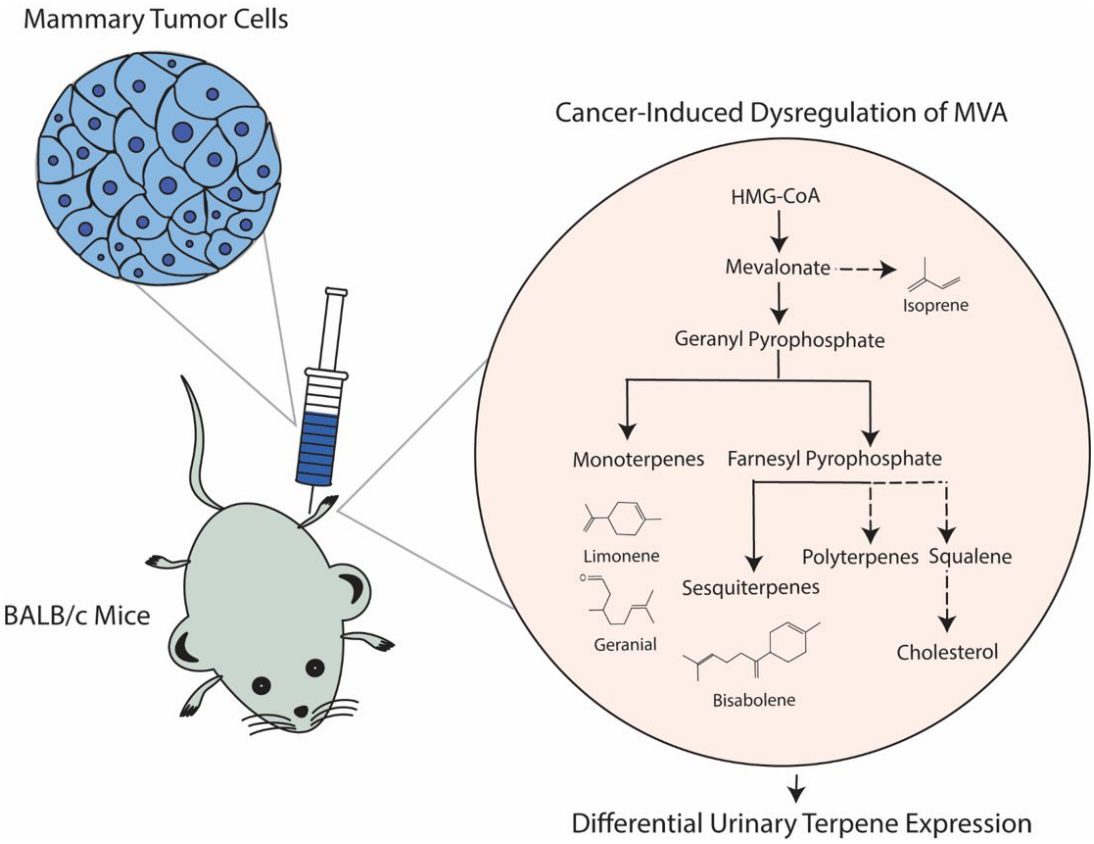

Figure 6. Schematic of murine tumor cell injection leading to the dysregulation of the mevalonate pathway highlighting VTs identified as altered in the localized tumor model (limonene and isoprene) and in the metastasized tumor model (bisabolene and geranial). (MVA = mevalonate, HMG-CoA = 5-hydroxy-3-methylglutaryl-coenzyme A reductase)